JOURNAL OF OPTOELECTRONICS AND ADVANCED MATERIALS Vol. 10, No. 10, October 2008, p. 2494 - 2501

Three dimensional numerical modeling and simulation of a uniformly doped GaAs MESFET photodetector

K. BALASUBADRA[a], T.THANGAM[b] , V. RAJAMANI[c*], K. SANKARANARAYANAN[d]
Department of Electronics and Communication Engineering
[a]*K.L.N.College of Information Techn., Sivagangai, TN, India - 630 611*
[b]*PSNA College of Engineering and Technology, Dindigul, Tamilnadu, India – 624 622.*
[c]*Indra Ganesan College of Engineering, Manikandam, Tiruchirappalli, TN, India - 620 012*
[d]*V.L.B. Janakiammal Engg. College, Coimbatore, TN, India - 641 042.*

A new 3D numerical model of a GaAs MESFET Photo detector has been presented in this paper. The model takes into account all the major effects that determine the device characteristics in the illuminated condition. It has been found that in a short channel MESFET photo detector, the drain current saturation is caused by the velocity saturation of the carriers rather than the pinch off condition. By considering both the photo conductive effect in the channel and photo voltaic effect at the gate schottky barrier, the major limitations of the existing model have been overcome. A three dimensional Poisson's equation has been solved with suitable boundary conditions to obtain the potential profile in the channel. The electric field profile along the length, width and thickness of the channel and mobility of the carriers have also been studied extensively under illuminated condition. Calculations are being carried out to examine the effect of illumination on the current-voltage characteristics, internal gate-to-source capacitance (C_{gs}), drain to source capacitance(C_{ds}), drain to source resistance (R_{ds}) and tranconductance(g_m) Due to effect of photo generation in the semi insulating substrate, the device characteristics are strongly influenced. The results of numerical calculations show that there is an increase in electron mobility and switching speed under the illumination condition. The proposed model is fairly accurate and can be used for accurate simulation of OptoElectronic Integrated Circuits (OEIC) using uniformly doped GaAs MESFET photo detector.

(Received January 1, 2008; accepted August 14, 2008)

Keywords: Device simulation, numerical 3D modeling, GaAs MESFET, Photo detector, OEIC

1. Introduction

Information technology has had an exponential growth through the modern telecommunication systems. Particularly, optical communication system play an vital role in the development of high quality and high speed communication systems. A new era in optical communication started after the invention of laser in 1960. Today optical communication systems not only used in telecommunication systems but also in Internets and Local Area Networks (LAN) to achieve high signaling rate.

Fig. 1 shows the basic components in fiber optical communication system. The input electrical signal modulates the light from the optical source. The optical carrier can be modulated internally or externally by electro-optic modulator or acousto-optic modulator. Now a days electro-optic modulators (KDP, $LiNbO_3$, beta barium borate) are widely used as external modulators which modulates the light by changing its refractive index through the given electrical signal.

In digital optical communication systems the input electrical signals is in the form of coded digital pulses from the encoder and these electric pulses modulates the intensity of light from the laser diode or LED and convert them into optical pulses. In the receiver stage, like FET photodetector or PIN diode converts the optical pulses into electrical signals. A large number of works has been reported concerning the use of field effect transistor in optically controlled amplification, oscillations and optical detection especially in Optoelectronic Integrated Circuit (OEIC) receivers. The optical circuits are advantageous because they can be integrated into the microwave circuits without interfering with them and they have low losses and small dimensions, short reaction time and wide band.

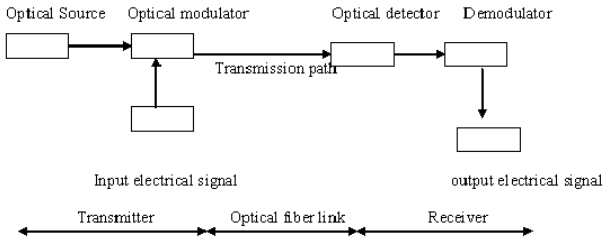

Fig. 1. Basic components of fiber optical communication system.

1.1. Modeling and Simulation

Integration of billions of transistors in a single chip beyond the year 2000 will require that the dimensions be reduced to below 0.1 micrometer levels. However, as the device dimensions are reduced, two- and three-dimensional electrostatic effects tend to degrade the

performance. Therefore, accurate, physical and analytical/numerical models are useful to predict the behavior of the small geometry semiconductor devices, and to give insights into device design and their scaling limits.

Modeling is probably the most intensive and time consuming part of the development process. Goal of the modeling process is to make sure that all the parameters that are needed for the characterization of the device are completely and accurately represented.

The electrical characteristics of the semiconductor devices are sensitive to the device structure and the operational condition due to the multi dimensional effects. In general, fundamental device modeling may provide some valuable information for understanding the physics of semiconductor devices. An accurate analytical model becomes difficult to develop because of the complexity of mathematical treatment for the multi dimensional effects and cannot be generalized for any device structure [1]. Therefore the device numerical simulation based on the self-consistent calculation of the semiconductor device equation has become important in device modeling.

Due to the mutual coupling effect between the Poisson's equation and the current continuity equation it is very difficult to develop an efficient solution for solving the full set of semiconductor device equation. For any device structure and bias condition, no method can guarantee to the stable and efficient in solving the semiconductor equations. From this point of view, the development of a fundamental solution method for the semiconductor equation is necessary to enhance the flexibility in the selection of an iteration algorithm.

3D models are necessary to address the geometric dependencies of such structure. It is almost impossible to deal analytically with certain problem like short channel effect or narrow width effect without resorting to some sort of assumptions or approximations. In numerical approach, the solution is readily available to any 2D or 3D problems such as short channel effect and narrow width effect. Therefore it is worth while to realize a device using a numerical device model to make a full use of the numerical model's accuracy in simulation [1].

1.2. Why MESFET Photodetector

METAL SEMICONDUCTOR FIELD EFFECT TRANSISTORS (MESFETs) have been looked upon for the applications in optical communication and optical computing as detector devices. Compound semiconductor field - effect transistors occupy an important niche in the electronic industry. An extremely important class of photo detectors involves the use of Schottky barrier produced between a metal and a lightly doped semiconductor.

The key advantage of Schottky barrier devices is that being a majority carrier device, it does not suffer from speed delays arising form minority carrier life time issues. In high-speed devices the depletion region is less than micron so that device speeds can be extremely high. With proper design Schottky barrier diodes can operate up to 160GHz. [2]. This detector is easy to fabricate and has an extremely high speed.

MESFETs has drawn considerable attention in recent years due to its potentiality as a good contender of MOSFET in VLSI/ULSI technology because of the following device characteristics: (1) enhanced radiation hardness, (2) immunity to hot carrier aging, (3) scaling well, and less mobility degradation [3] A high speed low power photo detector was first demonstrated experimentally by Baack et al [4]. Although Si-MESFETs are suitable for high speed applications GaAs MESFETs are more suitable than the former one for optical receivers. GaAs MESFETs are the most commonly used active devices in microwave circuits.

A number of theoretical and experimental works have been reported on GaAs MESFETs . The device is suitable for application in microwave monolithic integrated circuits (MMIC) and Optoelectronic Integrated circuits (OEICs) due to their integrated circuit compatibility.

The full exploitation of the information carrying capacity of the optical fibers needs the development of optical sources and detectors capable of handling data rates at such high rates [5-7]. The light induced voltage and the current characteristics of an optically controlled microwave device were reported analytically by Simons et al [5]. The switching characteristics of a high sensitivity GaAs MESFET for microwave ranges has been reported by Paolella et al [6]. The microwave circuit parameters of the GaAs MESFETs in the linear and saturation regions were experimentally reported by Gautier et al [7]. The response speed of 50 to 100ps with the photo conductive gain of 2 to 5 has been achieved with OPFET. The GaAs MESFETs can be used as a photodetector due to its higher carrier mobility and its potentiality. The optically controlled MESFET was named as Optical Field Effect Transistor (OPFET) and was introduced as a novel high speed optical detector by Gammel et al [8].

The 2-D potential distribution and threshold voltage for Si-SOI MESFETs for both uniform and non uniform was reported experimentally by Prashant Pandey et al. [9]. It provides a better understanding of the device. Hongliang Lv et al.[10] have reported the analytical model of I-V characteristics of MESFETs by considering multi parameter mobility. The drift velocity- field characteristics has been accurately obtained by Monte Carlo calculations. P.Chakrabarti et al [11] have reported the numerical simulations of an Ion –implemented GaAs OPFET. It has been used to compute accurately the various dc characteristics of device. P.Chakrabarti et al [12] reported a OEIC receiver based on MESFET Photo detector. The sensitivity of the OEIC receiver has been estimated for the above device.

This paper describes a 3D numerical simulation method for quantitative estimation of the performance of uniformly doped MESFET under illuminated condition. In order to understand and optimize the device characteristics with dimensions in the nanometer range, there is a need to develop a model for the potential distribution functions by solving the 3-D Poisson's equation. This paper provides a simple but fairly accurate model suitable for use in integrated optoelectronic circuit simulation purposes.

2. Theoretical modeling

The GaAs MESFET structure under consideration is similar to the conventional one except that the metal gate

has been assumed to the semi-transparent and is presented in Fig.2 This facilitates the transmission of radiation incident on the gate. For the present analysis, the epitaxial layer is considered to the uniformly doped with n-type material. The drain-to-source current flows in the horizontal x-direction and the incident optical radiation along vertical y-direction for the semitransparent metal gate. The incident radiation undergoes reflection at the metal gate entrance and is absorbed in the gate depletion region, render channel region, substrate depletion region, and bulk substrate region. Absorption of the radiation in the semiconductor results in the generation of excess electron hole pairs. These excess carriers change the charge distribution below the gate and the channel due to photoconductive effect. The minority carrier life time is decreased due to this excess carriers also cause a change in the built-in potential at the schottky contact and channel-substrate barrier due to a photo voltaic effect, and modulation the conductivity of the channel and enhances the substrate leakage current due to the photo conductive effect.

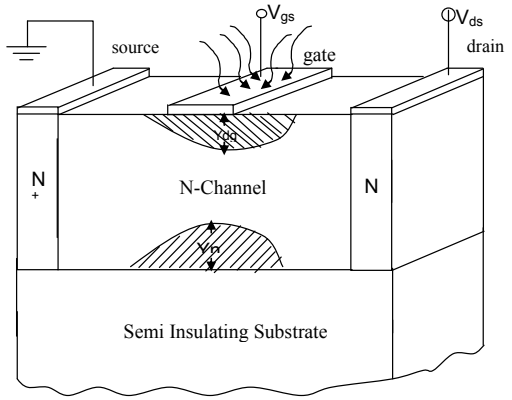

Fig. 2. Physical structure of GaAs MESFET photodetector.

In order to analyze the structure we need to solve both Poission's equation and current continuity equation. However, in the sub threshold regime, the currents are small and Poisson's equation alone is sufficient. The three-dimensional (3-D) Poisson's equation in the gate depletion region in the illuminated condition can be written as

$$\frac{\partial^2\psi(x,y,z)}{\partial x^2}+\frac{\partial^2\psi(x,y,z)}{\partial y^2}+\frac{\partial^2\psi(x,y,z)}{\partial z^2}=\frac{-q\left[N_d(y)+\frac{P_{opt}(1-R_m)(1-R_s)\alpha\tau_i e^{-\alpha y}}{h\upsilon}\right]}{\varepsilon_{si}\varepsilon_0} \tag{1}$$

where q is electron charge, ε_{si} is permittivity of silicon, ε_{so} is permittivity of free space, P_{opt} is incident optical power, R_m is reflection coefficient at entrance, Rs is reflection coefficient at metal contact, α is absorption coefficient, N_d is the uniform doping concentration and $\psi(x,y,z)$ is the potential at a particular point (x, y, z) in the gate, h is the Planck's constant, vis the frequency of the incident radiation, , τ_i is the mean lifetime of the minority carriers and q is the electron charge.

Boundary conditions required to solve the 3-D Poisson's equation can be written as

- Boundary conditions along the thickness of the device

$$\Psi\ (x, y, z)_{x=0} = V_{gs} - \varphi_{bi} \tag{2a}$$

$$\Psi\ (x, y, z)_{x=Leff} = V_{gs} - \varphi_{bi} \tag{2b}$$

- Boundary conditions along the length of the device

$$\Psi\ (x, y, z)_{y=0} = V_{bi} + V_{op} \tag{3a}$$

$$\Psi\ (x, y, z)_{y=teff} = V_{bi} + V_{ds} + V_{op} \tag{3b}$$

- Boundary conditions along the width of the device

$$\Psi\ (x, y, z)_{z=0} = V_{gs} + V_{bi} + V_{op} \tag{4a}$$

$$\Psi\ (x, y, z)_{z=weff} = V_{op} \tag{4b}$$

The source and the drain junction are located at y = 0 and y = L_{eff} , respectively, where L_{eff} is the effective channel length. The top and bottom ends are located at x = 0 and x = t_{eff} , where t_{eff} is the device thickness. The vertical and the lateral directions are defined as x , y respectively, while the direction along the width of the transistor is defined as z. The sidewall interfaces are located at z = 0 and z = $w_{eff.}$ Where V_{gs} is the gate to source voltage, V_{bi} is the built in potential between the channel to source junction and V_{op} is the photo induced voltage and V_{ds} is the drain to source voltage and φ_{bi} is the built in voltage of the Schottky barrier gate.

The excess carriers generated per unit volume (Δn) in the semiconductor due to the absorption of incident optical power density is given by,

$$\Delta n = \frac{\sqrt{1+\frac{4\tau P_{opt}(1-R_m)(1-R_s)(1-Ri)(1-e^{-\alpha W_m})}{W_m h\gamma n_i}}-1}{\frac{2P_{opt}(1-R_m)(1-R_s)(1-Ri)(1-e^{-\alpha W_m})}{W_m h\gamma n_i}} \tag{5}$$

where τ_i is the mean lifetime is the reflection coefficient at the insulator metal surface interface and W_m is the maximum width of the depletion layer and is given by

$$W_m = [4\varepsilon_s \ln(N_a / n_i) / q\beta N_a]^{1/2} \tag{6}$$

where, N_a is the acceptor concentration, ε_S is the permittivity of the semiconductor, $\beta = \frac{q}{kt}$, k being the Boltzmann's constant, T is the ambient temperature.

$G_{op}(y)$ is the excess carrier generation rate at any point y in the semiconductor and is given by

$$G_{op}(y) = \frac{p_{opt}}{h\gamma}(1-R_m)(1-R_i)(1-R_s)\alpha e^{-\alpha y} \tag{7}$$

The mean lifetime of the minority carriers in the illuminated condition, τ_I can be written as

$$\tau_l = (n_i / n_i + \Delta n)\tau \tag{8}$$

where, τ is the lifetime of the carriers for the intrinsic semiconductor.

In order to obtain electric field profile equations under dark and illuminated conditions (9a), (9b) and (9c) are solved respectively for the corresponding profiles in x, y and z directions.

The electric field in the respective directions is given by

$$E_{xph} = \frac{\Psi(i+1,j,k) - \Psi(i-1,j,k)}{2L / m_x} \tag{9a}$$

$$E_{yph} = \frac{\Psi(i,j+1,k) - \Psi(i,j-1,k)}{t / m_y} \tag{9b}$$

$$E_{zph} = \frac{\Psi(i,j,k+1) - \Psi(i,j,k+1)}{2W / m_z} \tag{9c}$$

where m_x, m_y and m_z are the separation of the grid line along the x and y directions .

The field dependent mobility have been obtained from

$$\mu_{xph} = \xi_S \xi_r E_{xph} \tag{10a}$$

$$\mu_{yph} = \xi_S \xi_r E_{yph} \tag{10b}$$

$$\mu_{zph} = \xi_S \xi_r E_{zph} \tag{10c}$$

where, ξ_S is the permittivity of the semiconductor, ξ_r is permittivity of the freespace and, E_{Xph}, E_{yph}, E_{Zph}, are the electric field in the x and y direction and the z direction respectively.

The drain current I_{dsph} due to illumination has been calculated by numerically integrating the charge in the channel region, given by

$$I_{dsph} = \frac{Z}{L} \int_0^{V_{ds}} \mu_n \left(E_{xph},\ E_{yph},\ E_{zph}\right) Q_n(V)\, dV \tag{11}$$

The charge in the neutral channel region $Q_n(V)$ under illumination has been computed by,

$$Q_n(V) = q \int_{y_{dg}}^{a} N_d(x,y)\, dy + q \frac{P_{opt}(1-R_m)(1-R_s)\alpha\tau_L}{h\nu} \int_0^a \exp(-\alpha y)\, dy \tag{12}$$

where, y_{dg} is the variation of depletion depth and function of potential distribution in the channel. The transconductance g_m and the gate to source capacitance (C_{gs}) under illumination condition can be estimated by

$$g_m \left\{v_{gs}(i)\right\}\Big|_{v_{ds};\ const} = \frac{I_{ds}(i+1) - I_{ds}(i-1)}{V_{ds}(i+1) - V_{ds}(i-1)} \tag{13}$$

$$C_{gs} = \left\{ V_{gs}(i) \Big|_{V_{ds};const} = \frac{Q_d(i+1) + Q_d(i-1)}{V_{gs}(i+1) - V_{gs}(i-1)} \right\} \tag{14}$$

The drain resistance, r_d and the responsivity of the device have been obtained from

$$r_d \left\{V_{ds}(i)\right\}\Big|_{V_{gs,const}} = \frac{V_{ds}(i+1,j) - V_{ds}(i-1,j)}{I_{ds}(i+1,j) - I_{ds}(i-1,j)} \tag{15}$$

$$R(\lambda) = \frac{I_{dsph} - I_{ds}}{P_{opt}} \tag{16}$$

where λ is the operating wavelength.

3. Computational techniques

The 3D Gaussian's distribution function is used to find the carrier concentration of the channel assuming the channel is uniformly doped. The calculated carrier concentration is verified by calculating the width of depletion layer both at the drain end and source end. The basic 3D Poisson's equation is solved using Liebmann's iteration method to determine the potential distribution through out the channel.

The channel profile has been obtained by dividing the channel region into several meshes as in Fig. 3. The potential distribution has been obtained by finding the potential at subsequent mesh points that are separated by 'm_x' along the vertical and 'm_y' along the lateral direction and 'm_z' along the width in discrete form as in equation (1) until the drain end of the gate is reached.

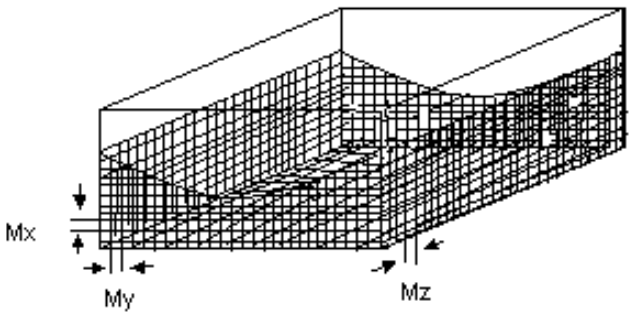

Fig. 3 Mesh model of the channel region.

The potential at every point in the channel and its variation along the length and width of the channel is calculated as

$$\psi(i,j,l)=\psi(i-1,j,l)+\psi(i+1,j,l)+\psi(i,j-1,l)+\psi(i,j+1,l)+\psi(i,j,l-1)+\psi(i,j,l+1)-((q(N_a+\Delta n)/\varepsilon_{si})/6) \quad (17a)$$

$$\psi(i,j,l)=\psi(i-1,j,l)+\psi(i+1,j,l)+\psi(i,j-1,l)+\psi(i,j+1,l)+\psi(i,j,l-1)+\psi(i,j,l+1)-((qN_a/\varepsilon_{si})/6) \quad (17b)$$

In order to solve a second-order differential equation of the form given by (1) the initial values of potential y is needed. An interactive approach has adopted to calculate these values with the help of available boundary conditions. The surface potential at the source end of the gate has been assumed to be zero. The potential at subsequent nodes toward drain end is calculated until the drain end of the gate is reached for an assumed value of drain-to-source current. The numerically estimated channel potential is used to calculate the electric field intensity along x,y and z directions and the electric field at every point is used to calculate the mobility of the carrier in all the three directions x,y,z. The drain current through the channel is obtained by solving Simson's rule. The computational flow diagram is shown in Fig.4.

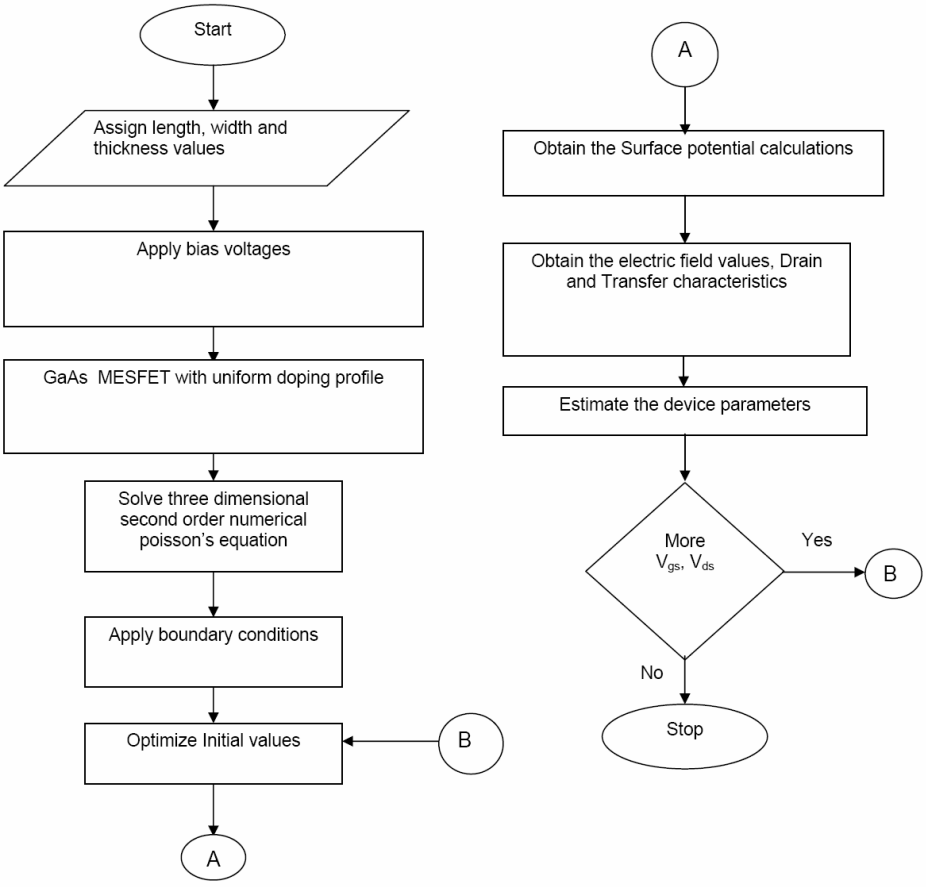

Fig. 4 Flowchart for the numerical simulation of GaAs MESFET photodetector

The current-voltage characteristics of the device have been obtained by the numerical integration for different values of drain-to-source voltage. The transfer characteristics of the device can be obtained by changing V_{gs} and computing the drain current for a given drain-to-source voltage by repeating the above method. The channel transconductance and gate-to-source capacitance (C_{gsph}) have been numerically obtained as a function of gate voltage or the illumination condition.

4. Results and discussion

Quantitative calculations of parameters have been carried out for a GaAs MESFET photo detector at 300K.The channel has been assumed to be uniformly doped with $N_d = 1.1\text{x}10^{23}/\text{m}^3$ .The gate length and the device width have been assumed to be 100nm and 40nm respectively. The depth of the channel has been assumed to be 80nm. The parameters used for calculating various values have been given in Table 1.

Table 1. The parameters used for computation.

Channel Length, L	100nm
Channel width, w	40nm
Device thickness, t	80nm
Absorption coefficient, α	10^6/m
Minority Carrier Life time, τ	10^{-8} s
Intrinsic carrier concentration, n_i	$1.79*10^{12}/m^3$
Built-in voltage of Schottky gate, φ_b	0.85V
Incident optical power, P_{OP}	0.2, 0.5W/ m^2
Reflection coefficient at entrance Rs	10% of Pop
Reflection coefficient at metal contact R_m	10% of Pop
Temperature, T	300K
Doping concentration, N_d	$1.1*10^{23}/m^3$
Gate voltage,V_{gs}	- 0.2 V
Drain voltage,V_{ds}	1V

As the drain of the n channel device is biased positively with respect to the gate, the gate depletion region is asymmetrically shifted towards the drain. Hence it is found that the potential decreases near the source end where as it linearly increases near the drain end. And also it is also proven that from Fig 5. The illuminated potential is slightly higher than that of the potential under dark condition due to the photo generated carriers (excess generated electron and hole pair).

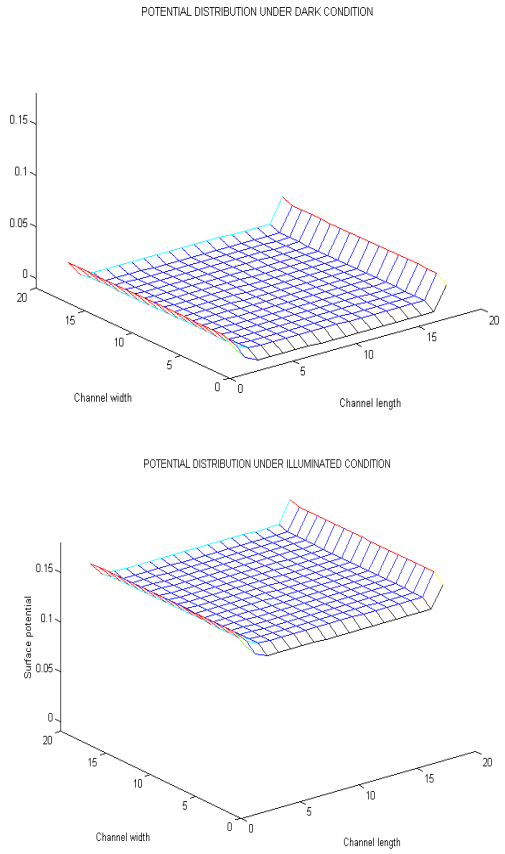

Fig.5. Potential Distribution in the channel under dark and illuminated condition.

Variation of electric fields under illuminated condition along the channel length and thickness has been obtained as shown in Fig. 6 and it is found that the electric field along the length of the channel is more dominant than electric field along the thickness of the device and also it is observed that the electric field increases rapidly near the drain end. Because the carrier density near the drain end experiences a rapid decrease in surface concentration which calls for a rapid increase in the electric field to maintain the constant drain current.

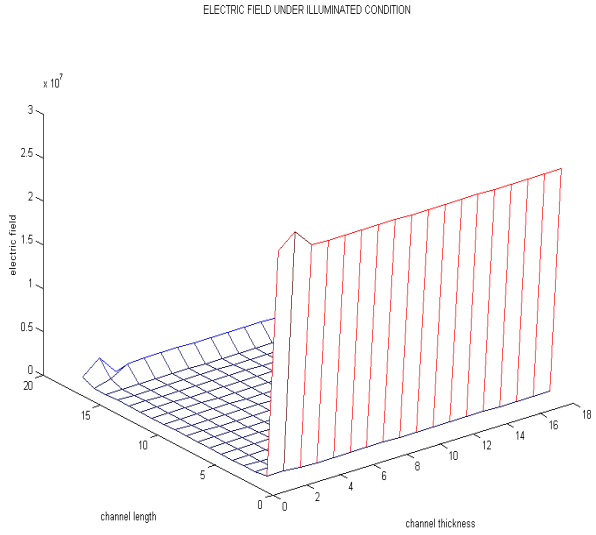

Fig.6. *Variation of electric field profile under Illuminated condition along the channel length and thickness*

Variation of electric field profile along the channel width (E_z) rapidly decreases near the drain end as opposite to that of E_y (along the length) as shown in Fig 7. This is due to the fact as if the V_{gs} applied at the gate side, the electron acquires more energy to move along the length of the channel.

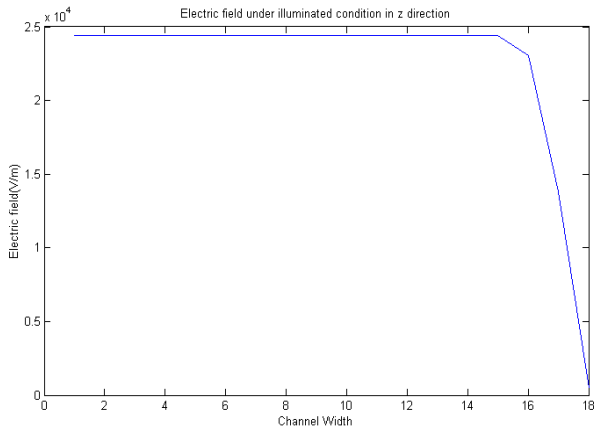

Fig.7. Variation of electric field profile under illuminated condition along the width of the channel

As field dependent mobility is directly proportional to the electric fields in their respective directions. Similar mobility profiles are obtained to that of the electric field profile as shown in Fig. 8 when an optical signal is illuminated on the device more and more electron hole pairs are generated. As the charge carriers are more crowded under illuminated condition, their mobility gets reduced in all three directions.

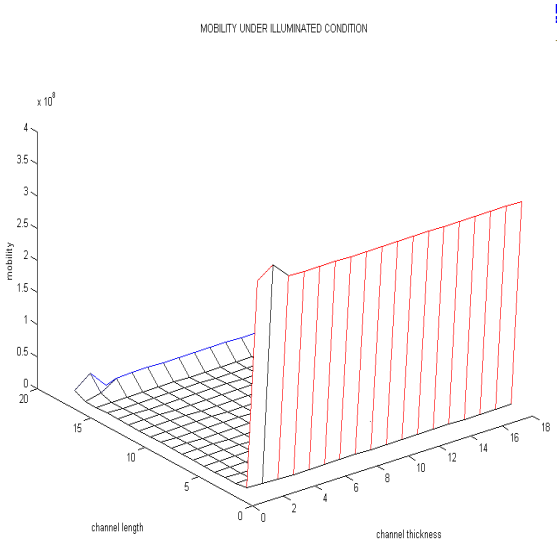

Fig. 8 Mobility distribution under illuminated condition along the channel length and thickness

It is seen that the as the applied drain-to-source voltage increases, the drain current initially increases significantly as shown in Fig 9. For the fixed value of V_{gs}= -0.2V. When drain voltage increases further, more charge carriers try to pass through the channel due to which drain current increases that is created earlier which is not enough. Hence the drain current saturates after a certain limit even if drain voltage is increased further.

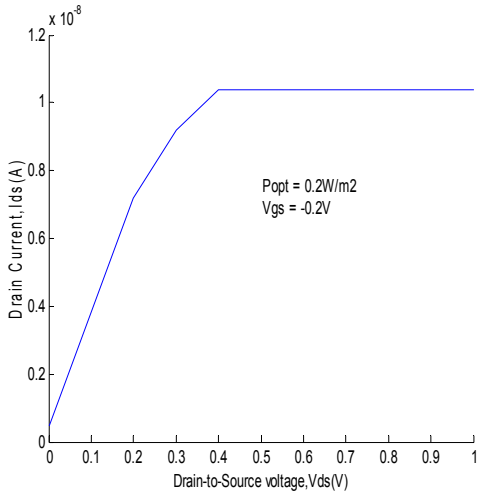

Fig 9. Variation of drain current under illumination conditions.

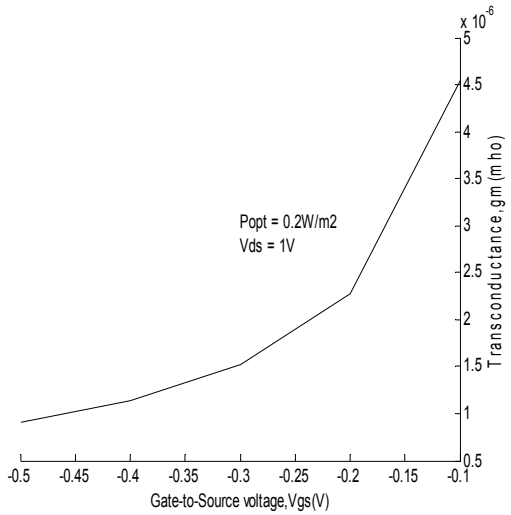

Fig 10. Transconductance in illumination condition

From Fig.10, it is observed that the transconductance of the device decreases with increase in the reverse voltage for a given V_{ds} and increases in the illuminated condition for a fixed V_{gs}. Also, the transconductance is affected by the source resistance. Beyond the saturation voltage the increasing value of V_{ds} does not affect the drain current and therefore the drain resistance has no further effect on the transconductance.

4. Conclusions

Device characteristics like potential distribution, field distribution and mobility distribution under dark and illuminated condition have been numerically estimated for uniformly doped GaAs MESFET. Other parameters such as drain characteristics, transfer characteristics, relationship between transconductance and gate voltage are also calculated numerically. It is seen that the device has all qualities to be used as a photo detector in OEIC receivers. The easy realization on GaAs MESFET provides accurate control on the gate length and channel thickness. The present work is confined to modeling and simulation of uniformly doped three dimensional GaAs MESFET photodetectors. The future work can be carried out with three dimensional non-uniform doping and also with multi dimensional analysis. The detailed noise analysis can also be carried out to develop an equivalent circuit model for the accurate characteristics of the device for the use in OEIC applications.

Acknowledgment

The authors are grateful to the All India council for Technical Education (AICTE), New Delhi, India for providing research grants (0023/BOR/RPS/080/06/07) in the year 2006-2007.

References

[1] S.P.Chin and C.Y.Wu, " A New Methodology for two dimensional Numerical Simulation of Semiconductor Devices", IEEE Trans. Computer Aided Design, **11**, pp. 1508-1521, (1992).

[2] P..Chakrabarti, N. L.Shrestha, S.Srivastava and V.Khemka, "An Improved Model of an Ion-implanted OPFET", IEEE Trans. Electron Dev., **39**, pp 2050-2059, Sept. (1992).

[3] S.M. Sze, "Physics of semiconductor Devices, 2nd Edition, Wiley Eastern Ltd., New Delhi, India, (1981).

[4] C. Baack, G.Elze and W.Walf, "GaAs MESFET: a high speed optical detector," Electron. Lett., **13**, p.193, (1977).

[5] Simons, R.N. and Bashin, K.B. "Analysis of optically controlled Microwave/Millimeter wave device structures", IEEE Trans. Microwave Theory and Tech., MTT 34, pp. 1349-1355, (1986).

[6] Paolella, A., Madjar, A. and Herezfeld, P.R., "Modelling of the GaAs V's response to modulated light at radio and microwave frequencies", IEEE Trans. Microwave Theory and Tech., MTT **42**, pp.1122-1130, (1994).

[7] Gautier, J.L., Pasquet, D., and Pouvil, P., "Optical Effects On the Static and Dynamic characteristics of a GaAs MESFET", IEEE Trans. Microwave Theory and tech., MTT **33**, pp. 819 – 822, (1985).

[8] J.C.Gammel and J.M.Ballantyne,"The OPFET : A new high speed optical detector," IEEE Int. Electron Dev. Meet. Dig., pp.120-123, (1978).

[9] Prashant Pandey and B.B.Pal, "A New 2D Model for the Potential Distribution and Threshold Voltage of Fully Depleted Short-Channel Si -SOI MESFET's", IEEE Transaction Electron Devices, **51**, pp.246-254, (2004).

[10] Hongliang Lv, Yimen Zhang , Yuming Zhang and Lin-An Yang," Analytic Model of I_V Characteristic of 4H-SiC MESFETs Based on multi parameter Mobility Model", IEEE Transaction on Electron Devices, **51**, pp.1065-1068, (2004).

[11] P. Chakrabarti, M. Madheswaran, A. Gupta and N.A Khan , "Numerical Simulation of an Ion-Implanted GaAs OPFET", IEEE Trans. Microwave Theory & Tech., MTT **46**, pp.1360-1365, (1998).

[12] P.Chakrabarti and V.Rajamani, "A Proposed OEIC Receiver Using MESFET Photodetector", IEEE J. Lightwave Technology, vol.12, pp.659-668, (1999).

* Corresponding author: rajavmani@gmail.com,
rajavmani@rediffmail.com